Pain 121 (2006) 219–231

PAIN

www.elsevier.com/locate/pain

Activation of glia and microglial p38 MAPK in medullary dorsal horn contributes to tactile hypersensitivity following trigeminal sensory nerve injury

Zheng Gen Piao [a,1], Ik-Hyun Cho [a,1], Chul Kyu Park [a], Jin Pyo Hong [a], Se-Young Choi [a], Sung Joong Lee [a], Seungbok Lee [b], Kyungpyo Park [a], Joong Soo Kim [a], Seog Bae Oh [a,b,*]

[a] *Department of Physiology, College of Dentistry and Dental Research Institute, Seoul National University, Seoul 110-749, Republic of Korea*
[b] *Program in Molecular and Cellular Neuroscience, College of Dentistry and Dental Research Institute, Seoul National University, Seoul 110-749, Republic of Korea*

Received 19 May 2005; received in revised form 1 December 2005; accepted 19 December 2005

Abstract

Glial activation is known to contribute to pain hypersensitivity following spinal sensory nerve injury. In this study, we investigated mechanisms by which glial cell activation in medullary dorsal horn (MDH) would contribute to tactile hypersensitivity following inferior alveolar nerve and mental nerve transection (IAMNT). Activation of microglia and astrocytes was monitored at 2 h, 1, 3, 7, 14, 28, and 60 days using immunohistochemical analysis with OX-42 and GFAP antibodies, respectively. Tactile hypersensitivity was significantly increased at 1 day, and this lasted for 28 days after IAMNT. Microglial activation, primarily observed in the superficial laminae of MDH, was initiated at 1 day, maximal at 3 days, and maintained until 14 days after IAMNT. Astrocytic activation was delayed compared to that of microglia, being more profound at 7 and 14 days than at 3 days after IAMNT. Both tactile hypersensitivity and glial activation appeared to gradually reduce and then return to the basal level by 60 days after IAMNT. There was no significant loss of trigeminal ganglion neurons by 28 days following IAMNT, suggesting that degenerative changes in central terminals of primary afferents might not contribute to glial activation. Minocycline, an inhibitor of microglial activation, reduced microglial activation, inhibited p38 mitogen-activated protein kinase (MAPK) activation in microglia, and significantly attenuated the development of pain hypersensitivity in this model. These results suggest that glial activation in MDH plays an important role in the development of neuropathic pain and activation of p38 MAPK in hyperactive microglia contributes to pain hypersensitivity in IAMNT model.

Keywords: c-Fos; GFAP; Glia; Inferior alveolar nerve; Medullary dorsal horn; Mental nerve; Minocycline; OX-42; p38 mitogen-activated protein kinase; Tactile hypersensitivity

1. Introduction

Glial cells (microglia and astrocytes) in the central nervous system (CNS) respond to the peripheral insults. As determined by upregulation of glial cell markers, both microglia and astrocytes are activated following peripheral nerve injuries such as nerve transection, ligation, and crush (Garrison et al., 1991; Kalla et al., 2001), and chemical insult (Fu et al., 1999). The glial cell activation could simply reflect the pathological responses elicited by peripheral nerve injury, as with glial cell responses in CNS induced by insults to brain or spinal cord (Kreutzberg, 1996; Aschner, 1998). However, given that glial activation

* Corresponding author. Tel.: +82 2 740 8656; fax: +82 2 762 5107.
E-mail address: odolbae@snu.ac.kr (S.B. Oh).
[1] These authors contributed equally to this work.

0304-3959/$32.00
doi:10.1016/j.pain.2005.12.023

following peripheral sensory nerve injury is directly correlated with pain facilitation such as hyperalgesia and allodynia observed in these animals (Sweitzer et al., 1999; DeLeo and Winkelstein, 2002; Winkelstein and DeLeo, 2002), glial cell activation might play a more active physiological role, rather than simply reflecting these pathologic conditions (Zimmermann, 2001). Indeed, a wealth of studies demonstrate the positive correlation between spinal glial activation and the development or maintenance of pain hypersensitivity (Watkins and Maier, 2003; Tsuda et al., 2005). Accordingly, the current lack of appropriate treatment of neuropathic pain might be attributable to the limited understanding on the role of glial cells in pathological pain (Watkins and Maier, 2002, 2003).

Based on these findings, the detailed mechanisms by which the interaction between glial cells and spinal neurons eventually induce pathological pain, which are clearly different from those of acute nociceptive pain processing, are now under extensive investigation (Bursztajn et al., 2004; Ohtori et al., 2004; Tsuda et al., 2004). Although clinical studies indicate that neuropathic pain is more frequently observed in the trigeminal system than at the spinal level (Sweet, 1984), most current studies use the injury models of spinal sensory nerve rather than those of orofacial regions (Winkelstein and DeLeo, 2002; Inoue et al., 2003). Several animal models with injuries to the infraorbital nerve or inferior alveolar nerve (Vos et al., 1994; Nomura et al., 2002; Yonehara et al., 2003) have been demonstrated to exhibit mechanical or thermal hypersensitivity. However, the involvement of glial cell activation in the pain hypersensitivity in these animals is still yet to be determined.

In the present study, we set out to clarify the role of glial cell activation in the trigeminal neuropathic pain. For this purpose, we investigated whether the tactile hypersensitivity would correlate with the activation of glial cells in a trigeminal neuropathic pain model, which was created via the transection of both inferior alveolar nerve (IAN)[2] and mental nerve (MN). The activation of microglia and astrocytes was immunohistochemically determined by OX-42 and glial fibrillary acidic protein (GFAP) antiserum, respectively, after identifying the distribution of medullary dorsal horn (MDH) neurons activated by inferior alveolar nerve and mental nerve transection with c-Fos immunostaining. Finally, we examined mechanisms by which microglial activation contributes to the development of pain hypersensitivity in this model.

[2] *Abbreviations used:* GFAP, glial fibrillary acidic protein; IAN, inferior alveolar nerve; IAMNT, inferior alveolar and mental nerve transection; IR, immunoreactivity; MDH, medullary dorsal horn; MN, mental nerve; MAPK, mitogen-activated protein kinase; TG, trigeminal ganglion.

2. Materials and methods

2.1. Animals

All surgical and experimental procedures were reviewed and approved by the Institutional Animal Care and Use Committee (IACUC) in College of Dentistry, Seoul National University. Animal treatments were performed according to the Guidelines of the International Association for the Study of Pain (Zimmermann, 1983). Male Sprague–Dawley (SD) rats (approximately weighing 180–200 g at the time of surgery) were used. Rats were housed at a temperature of 23 ± 2 °C with a 12-h light–dark cycle (light on 08:00 to 20:00), and fed food and water ad libitum. The animals were allowed to habituate to the housing facilities for 1 week before the experiments, and efforts were made to limit distress to the animals.

2.2. Surgery and experimental groups

Rats were randomly assigned to one of four groups; (1) rats with inferior alveolar nerve and mental nerve transection (IAMNT) ($n = 80$), (2) sham-operated rats ($n = 35$), and (3) normal control rats ($n = 20$), and (4) minocycline-treated rats ($n = 33$). Rats were anesthetized with sodium pentobarbital (30 mg/kg, i.p.). For IAMNT rats, the facial skin over the left masseteric muscle was cut and the mandibular bone was exposed, the bone surface over the IAN/MN (two distal branches of mandibular nerve) was carefully removed, and both the IAN and MN were exposed. The left IAN and MN were transectioned where the nerve trunk lies just beneath the coronoid process, and cutaneous tissues were then sutured. For sham-operated rats, exposure of the left IAN/MN was performed without nerve transection. The contralateral sides were left intact in all rats. Minocycline (15 or 30 mg/kg, Sigma–Aldrich, USA) or saline vehicle was injected intraperitonially (i.p.) 1 h before IAMNT and continued daily to day 14 after IAMNT. No post-operative treatment such as antibiotics was given to the operated rats.

2.3. Behavioral experiments

Behavioral tests were carried out 2 days before surgery, and 1, 3, 7, 14, 28, and 60 days after surgery under constant condition (temperature, 23 ± 2 °C; humidity, $55 \pm 5\%$) between 9:00 am and 12:00 am in a quiet room. A series of von Frey filaments (Semmes-Weinstein Monofilaments, North Coast Medical, Inc., USA) were used to determine pain hypersensitivity to mechanical stimulation (Yonehara et al., 2003). To observe behavioral response to the mechanical stimulation, individual rat was placed in a plastic cage ($25 \times 40 \times 18$ cm) without bedding. After the rats were accommodated for 30 min, von Frey filaments (bending force; 0.008, 0.02, 0.04, 0.07, 0.16, 0.4, 0.6, 1.0, 1.4, 2.0, 4.0, and 6.0 g) were delivered from above to the center of whisker pad. Each von Frey filament was applied five times to the same region at approximately 5 s intervals. Head withdrawal, touching or scratching the facial regions upon von Frey filament applications was considered as positive pain response. A recovery (5 min) was allowed to rats after each threshold was obtained. The response threshold was defined as the lowest force of the filaments that produced at least three positive responses in five trials. We excluded the rats that either

responded to 0.008 and 0.02 g (>3 out of 5 trials) or did not respond to 6.0 g (>3 out of 5 trials). The threshold for escape behavior in response to mechanical stimulation was measured in the three groups of rats (saline-, minocycline-treated IAMNT rats, and sham-operated rats).

2.4. Immunohistochemical staining in the medullary dorsal horn (MDH)

Rats were perfused with physiological saline and sequentially with fresh 4% paraformaldehyde in 0.1 M phosphate buffer (pH 7.4) at 2 h and 1, 3, 7, 14, 28, and 60 days after IAMNT. The caudal medulla and upper cervical spinal cord were removed as one block and were immersed in the same fixative at 4 °C overnight and then transferred to 30% sucrose in PBS for 48 h. Serial frozen transverse sections (30 μm thickness) were made through the caudal medulla and first segment of the spinal cord (Cl), collected in cold PBS. All immunohistochemical procedures were performed at room temperature (RT) unless otherwise stated. Free-floating sections were incubated for 30 min with 3% H_2O_2 in 0.1 M PBS (pH 7.4) to remove endogenous peroxidase activity, washed in PBS, and then kept by blocking solution containing 5% normal goat/or horse serum, 2% BSA, 2% FBS, and 0.1% Triton X-100 for 2 h at RT. The sections were incubated overnight at 4 °C with either rabbit anti-c-Fos (1:10,000; Oncogene, USA), mouse anti-OX-42 (CDllb/c) (1:2,000; Cedarlane, Canada), or rabbit anti-GFAP antibody (1:10,000; DAKO, Denmark), and washed in PBS. Sections were then incubated with biotinylated secondary antibodies (Vector Laboratories, USA), respectively, at a dilution of 1:200 for 1 h, followed by incubation with avidin and biotinylated HRP complex (Vector Laboratories, USA) at 1:200 for 1 h and visualized with 3,3′-diaminobenzidine (D-5637; Sigma, USA). The immunostained sections were mounted onto gelatin-subbed glass slide, dehydrated through a series of ethanol, cleared, and coverslipped with permount. For double immunofluorescent staining, floating sections were incubated overnight at 4 °C with a mixture of rabbit anti-phospho p38 MAPK antibody (1:500; Cell signaling, USA) and mouse anti-OX-42 antibody (1:1000), mouse anti-NeuN antibody (1:2000; Chemicon, USA) or mouse anti-GFAP antibody (1:50; Chemicon, USA). The sections were then incubated for 1 h at RT with a mixture of FITC- and Cy3-conjugated rabbit/mouse IgG antibody (1:200; Jackson ImmunoResearch, USA). The sections were mounted with VectaShield (Vector Laboratories, USA).

2.5. Retrograde labeling and counting the number of trigeminal ganglion (TG) neurons

Trigeminal ganglion (TG) neurons were retrograde-labeled with a fluorescent dye, Dil (Molecular Probes, OR, USA). Briefly, left IAN and MN were transected as described above. At 2 days before the designated time points (3, 7, 14, 28, and 60 days after IAMNT), Dil was placed onto the proximal end of the transected IAN/MN nerve ($n = 5$/group). For control rats, application of the Dil was performed just following IAN/MN nerve transection. A parafilm was placed on Dil to prevent spread of leaked tracer. The skin was then sutured and the rats were allowed to recover. At the designated time points, rats were perfused and TG was processed as described above. Serial frozen longitudinal sections of TG (20 μm thickness) were mounted on gelatin-coated slides. All Dil-labeled TG neurons were counted from one section per every 100 μm thickness interval under fluorescent microscope.

2.6. Data analysis

Trigeminal spinal nucleus complex was located with cresyl violet staining (see supplementary data). The middle portion of trigeminal spinal nucleus interpolaris (Vi)-trigeminal spinal nucleus caudalis (Vc) border, which corresponds to the level of obex, was defined as the rostro-caudal zero (0) point. Upper and lower positions were presented as + or −, respectively, in the range from +1.2 to −6.0 mm. Like spinal dorsal horn, this nucleus has a laminar structure (therefore called as medullary dorsal horn, MDH), and the regions between the borders of laminae roughly correspond to the location of neurons with different functions. Thus, based on cytoarchitectural and functional criteria, the MDH was divided into two regions as follows: (1) the superficial layer, including laminae I and II; (2) the deep laminae, including laminae III and IV. The images of stained sections were captured using image system (KAPPA ImageBase DX 30, KAPPA opto-electronic Inc., USA) under light microscope. The boundaries between these two regions were drawn according to previously described criteria (Strassman and Vos, 1993) (Fig. 2B). The expression of c-Fos was quantified by counting c-Fos immunoreactive (c-Fos-IR) cells in the trigeminal spinal nucleus caudalis (Vc). The number of c-Fos positive cells from four sections was analyzed every 1.2 mm from the trigeminal spinal nucleus interpolaris (Vi) and caudalis (Vc) border to Cl region at both sides of the MDH. The total number of c-Fos positive cells from four rats in each group was averaged and then analyzed.

Evaluation of microglial and astrocytic activation was scored blinded to experimental conditions using captured images. At least four sections at each level were used to determine scoring for each animal. The specific morphological changes of the OX-42 and GFAP positive cells were scored as follows: no response (−), mild response (+), moderate response (++), and intense response (+++). The criteria for each score have been described in detail previously (Colburn et al., 1997). In brief, ''activation response'' scoring is based on the observed cell morphology, local cell density, and intensity of OX-42 and GFAP immunoreactivity.

The double-stained images for p-p38 or OX-42 were analyzed using confocal laser scanning microscopy (LSM 5 PASCAL; Carl Zeiss, Germany). To quantify the changes in immunofluorescence intensity of the p-p38 or OX-42 expression in the MDH after IAMNT, we measured the average pixel intensity per 0.5 mm^2 area within medial portion of the superficial and deep laminae of the MDH of four sections at the level of 2.4 mm caudal to obex 3 days after IAMNT.

To minimize variability in staining, the tissue from all groups was processed following the same immunohistochemical condition. Extreme care was taken to analyze the same regions of the Vc-C1 to minimize differences due to anatomical variation.

2.7. Statistics

All results are expressed as mean ± SEM. Student's *t*-test was used to verify the change in the number of c-Fos-immunoreactive cells and Dil-labeled TG neurons. For multiple comparison, the statistical significance of the difference was assessed with an analysis of variance (ANOVA) followed by post hoc Newman–Keuls test. Differences were considered to be significant when *P* value was less than 0.05.

3. Results

3.1. Behavioral response to IAMNT

Two days before IAMNT, the withdrawal threshold to mechanical stimulation of the whisker pad was measured to monitor the control threshold. The withdrawal threshold was indicated as the relative value to the preoperative withdrawal threshold (sham-contra, 0.72 ± 0.03 g; sham-ipsi, 0.69 ± 0.24 g; IAMNT-contra, 0.77 ± 0.09 g; IAMNT-ipsi, 0.78 ± 0.20 g). Fig. 1 illustrates the behavioral response upon the mechanical stimulation to the whisker pad in IAMNT rats and sham-operated rats. The withdrawal threshold upon the mechanical stimulation of the whisker pad to the ipsilateral side to IAMNT was significantly decreased from 1 day after surgery (1 day, 0.35 ± 0.09 g; 3 days, 0.09 ± 0.02 g; 7 days, 0.11 ± 0.04 g; 14 days, 0.08 ± 0.02 g). The threshold decrease lasted through 28 days (0.15 ± 0.04 g) following IAMNT and returned to the basal level by 60 days (0.28 ± 0.20 g). We did not observe significant differences in withdrawal threshold on the contralateral side of IAMNT rats, or the ipsilateral or the contralateral side of sham-operated rats (Fig. 1). These data indicate that IAMNT provides a valid neuropathic pain model in orofacial area. Therefore, we set out further experiments to determine the role of MDH glia in our trigeminal neuropathic pain model.

3.2. c-Fos response to IAMNT

Because c-Fos is a neuroactive marker that can be used to analyze nociceptive pathways (Terayama et al., 1997; Nomura et al., 2002), we located the areas in MDH activated by IAMNT. In three animal groups assigned in our study, a small number of c-Fos positive neurons were widely found not only in trigeminal spinal sensory nuclei complex but also in several other brainstem areas such as the reticular nucleus (RN) and solitary nucleus (data not shown). We only analyzed c-Fos positive cells in MDH where primary nociceptive afferents from mandibular nerve terminate, since c-Fos expression in areas other than MDH was not likely to be directly related with the tactile hypersensitivity following IAMNT. As illustrated in Fig. 2, IAMNT increased c-Fos expression in ipsilateral MDH (Figs. 2B and E). However, only a modest number of c-Fos positive neurons was found on either side of sham-operated (Fig. 2C), or the contralateral side of IAMNT, rats (Figs. 2A and D). IAMNT-induced c-Fos expression was predominant in the superficial laminae (I–II) and deep laminae (III–IV) of the ipsilateral MDH, and mainly restricted to the dorsomedial one-third of MDH (Figs. 2B and E). In all control, sham-operated, and experimental groups, c-Fos positive neurons were only rarely found in both the ipsilateral and contralateral sides beyond +1.2 mm.

When we examined the temporal changes in c-Fos expression from 2 h to 60 days in the both ipsilateral and contralateral sides from IAMNT rats, significant temporal changes in c-Fos expression in superficial laminae were found on the ipsilateral side, whereas the c-Fos expression levels in the superficial laminae were similar between the contralateral MDH of the IAMNT rats and both sides of the sham-operated rats (data not shown). The representative rostro-caudal (from +1.2 to −6.0 mm) distribution of c-Fos positive cells at 1, 7 and

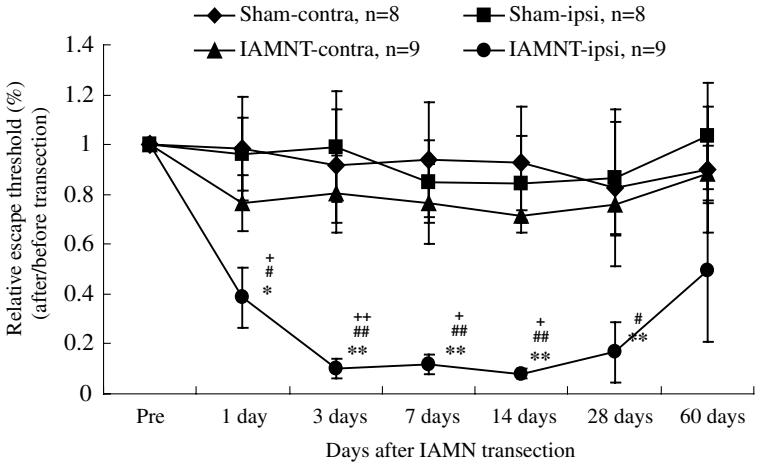

Fig. 1. Changes in the escape thresholds to noxious mechanical stimulation in the whisker pad area of the sham-operated and IAMNT rats. Sham-contra/ipsi, contralateral/ipsilateral side to sham-operated rats; IAMNT-contra/ipsi; contralateral/ipsilateral side to the IAMNT rats. (Newman–Keuls test; $^{*,\#,+}p < 0.05$; $^{**,\#\#,++}p < 0.01$; ∗, saline-ipsi vs. pre-operative (Pre); #, saline-ipsi vs. saline-contra; +, saline-ipsi vs. sham-ipsi or contra).

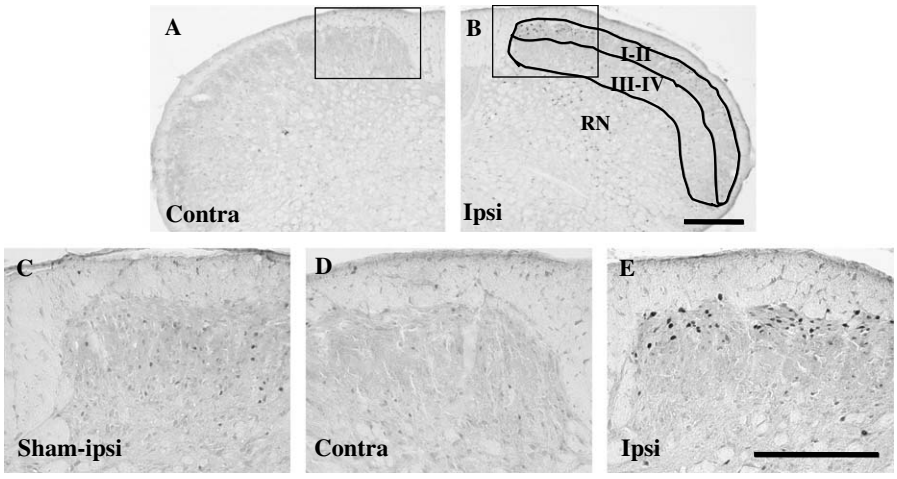

Fig. 2. The representative photograph showing c-Fos-immunoreactivity (IR) of medullary dorsal horn (MDH) (at 2.4 mm caudal from obex) at 2 h after transection of both inferior alveolar nerve and mental nerve (IAMNT). c-Fos positive cells were mainly found in the dorsomedial one-third in the superficial laminae (I–II) of the ipsilateral MDH. (A) Contralateral side to IAMNT, (B) ipsilateral side to IAMNT. (C) ipsilateral side to sham operation. (D and E) High magnification of the open rectangles in (A) and (B). The scale bar in (B) and (E) indicates 500 and 100 μm, respectively.

28 days is shown in Fig. 3. Following IAMNT, the c-Fos expression peaked at 2 h and 1 day (Figs. 3A and B), and a significant number of c-Fos positive cells were still detected in the superficial laminae on the ipsilateral side at 3 days (data not shown), 7 days (Figs. 3C and D), and 14 days (data not shown). However, the total number of c-Fos positive cells then gradually decreased by 28 days (Figs. 3E and F) and returned to the basal level at 60 days after IAMNT. The differences in c-Fos expression between the ipsilateral and contralateral side were also

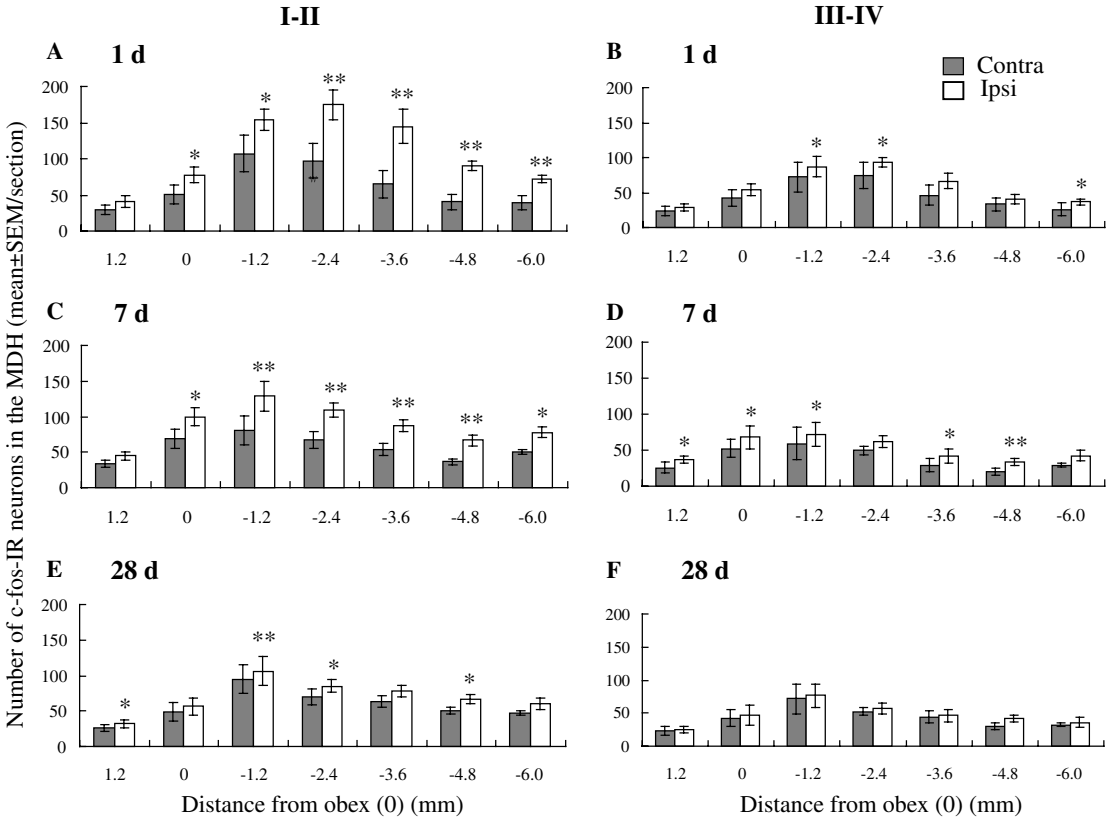

Fig. 3. Rostro-caudal distribution of c-Fos-IR in the superficial laminae (I–II) and deep laminae (III–IV) of the ipsilateral MDH at 1 day (A and B), 7 days (C and D), and 28 days (E and F) following IAMNT. ($n = 4$/group). (A, C, and E), I–II; (B, D, and F), III–IV. (Student's t-test; $^{*}p < 0.05$; $^{**}p < 0.01$; ipsilateral of IAMNT rats vs. contralateral of IAMNT rats).

significant at 2 h, 1, 7 and 14 days, and even 28 days, although the difference was much greater at the earlier time points. However, due to the gradual decrease in the number of c-Fos expression, no significant difference in the number of c-Fos positive cells was observed between the ipsilateral and contralateral side at 60 days (data not shown). The pattern of temporal changes in the number of c-Fos positive cells in the deep laminae (III–IV) after IAMNT was similar to that of the superficial laminae, but with a smaller number of c-Fos positive cells (Figs. 3B, D, and F).

In summary, the largest number of c-Fos IR cells was expressed in the superficial laminae of the ipsilateral side of the Vc-C1 (between obex and −6.0 mm) at 2 h and 1 day after IAMNT.

3.3. Microglial response to IAMNT

Activated microglial cells in MDH were visualized by anti-OX-42 (CDllb/c) immunostaining. In both the contralateral side of IAMNT rats and the ipsilateral side of the sham-operated rats, OX-42 immunoreactivity (OX-42-IR) was uniformly distributed, but modest in intensity throughout MDH. The stained resident microglia had long finely branched processes that extended in all directions from the perinuclear cytoplasm (Figs. 4A and B). However, in the ipsilateral side, microglia had profound OX-42-IR after IAMNT and appeared to be in an activated state with enlarged cell bodies, and much shorter and thicker processes (Figs. 4D–H). OX-42-IR in ipsilateral MDH at 2 h after IAMNT (Fig. 4C) was comparable to those of contralateral side of IAMNT rats and the ipsilateral side of the sham-operated rats (Figs. 4A and B). However, the activated microglial cells were slightly increased throughout the superficial laminae of the ipsilateral side at 1 day after IAMNT (Fig. 4D, Table 1). The OX-42-IR was markedly increased at 3 days and maintained up to 7 days (Figs. 4E and F, Table 1). However, OX-42-IR was somewhat reduced at 14 and 28 days (Figs. 4G and H, Table 1), and became similar to that in the contralateral side by 60 days after IAMNT (Fig. 4I and Table 1). In contrast to that in the superficial laminae, OX-42-IR was mildly expressed in the deep laminae of the ipsilateral side after IAMNT (data not shown).

The spatio-temporal changes in OX-42 IR are given in Table 1. Interestingly, the microglial activation was found to occur approximately at the same area showing c-Fos upregulation (Fig. 2). Like c-Fos expression, the most extensive expression of activated microglia after IAMNT was observed in the medial portion of superficial laminae between 0 and −6.0 mm, and microglial activation was not found beyond +1.2 mm in either the ipsilateral or the contralateral side of all normal, sham-operated, or IAMNT groups.

3.4. Astrocytic response to IAMNT

Activated astrocytes were visualized with anti-GFAP immunostaining. GFAP immunoreactivity (GFAP-IR) in MDH was homogeneous, but modest throughout the superficial and deep laminae of ipsilateral side of the sham-operated rats and contralateral side of IAMNT rats, suggesting that astrocytes in these areas appeared to be in a resting state (Figs. 5A and B). Astrocytic activation was very mild beyond +1.2 mm in either the ipsilateral or contralateral sides of all normal, sham-operated, or experimental groups.

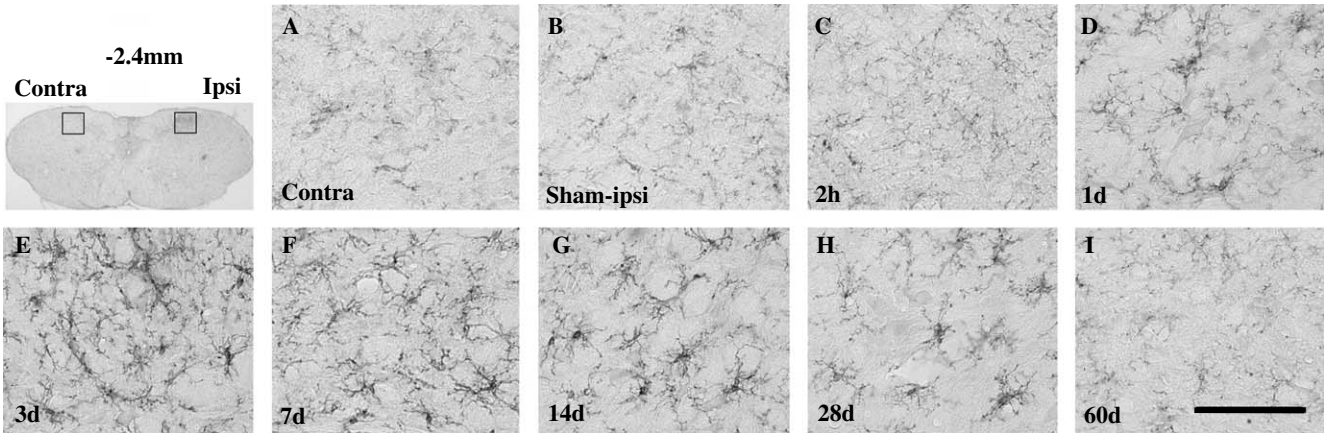

Fig. 4. OX-42 IR in the superficial laminae of the medullary dorsal horn following IAMNT at the level of 2.4 mm caudal to obex. (A–I) The magnified image of the inset indicated in the left top panel. (A) Contralateral side at 3 days after IAMNT. (B) Ipsilateral side at 3 days after sham operation. (C–I) Ipsilateral side at 2 h, 1 day, 3 days, 7 days, 14 days, 28 days, and 60 days after IAMNT, respectively. OX-42 IR was intense at 3 and 7 days with many hypertrophic microglia (E and F), and moderate at 14 days after IAMNT (G), whereas mild with several less ramified microglia at 1 day and 28 days after IAMNT (D and H). OX-42 IR at 2 h and 60 days after IAMNT (C and I) was very mild, which was comparable to those in the contralateral side (A) and the sham-ipsilateral side (B). Scale bar = 100 μm.

Table 1
Glial responses following inferior alveolar nerve and mental nerve (IAN/MN) transection

	Distance (mm)	OX-42							GFAP						
		2 h	1 day	3 days	7 days	14 days	28 days	60 days	2 h	1 day	3 days	7 days	14 days	28 days	60 days
IAMNT (ipsi)	+1.2	–	–	+	–	–	–	–	–	–	+	+	+	–	–
	Obex(O)	–	–	++	++	+	–	–	–	–	+	+	+	–	–
	−1.2	–	+	+++	++	+	+	–	–	–	++	+++	++	+	–
	−2.4	–	+	+++	+++	++	+	–	–	+	+++	+++	+++	+	–
	−3.6	–	–	++	+	+	+	–	–	–	++	++	+	+	–
	−4.8	–	+	+++	++	++	+	–	–	+	+++	+++	+++	+	–
	−6.0	–	+	+++	++	+	–	–	–	–	++	+++	++	+	–
IAMNT (contra)	+1.2 to −6.0	–	–	–	–	–	–	–	–	–	–	–	–	–	–
Sham (ipsi)	+1.2 to −6.0	–	–	–	–	–	–	–	–	–	–	–	–	–	–

Glial activation response scores were based on cell morphology, cell density, and intensity of immunoreactivity to OX-42 and GFAP.
Scores: not response (−), mild response (+), moderate response (++), and intense response (+++).

However, the ipsilateral side between 0 and −6.0 mm had strong GFAP-IR following IAMNT, and these cells had hypertrophic cell bodies and processes (Figs. 5D–H). Similar to the microglial responses, astrocytes appeared normal at 2 h and normal to mild at 1 day following the IAMNT (Figs. 5C and D, Table 1). However, moderate to intense astrocytic responses were discernible in IAMNT animals at 3, 7, and 14 days (Figs. 5E–G, Table 1), and mild to moderate astrocytic response was observed at 28 days post-IAMNT (Fig. 5H, Table 1). At 60 days post-IAMNT, astrocytes were similar to those of the contralateral MDH (Fig. 5I, Table 1).

In summary, the largest number of astrocytic activation was observed in the medial portion of the superficial laminae of the ipsilateral side where we found the upregulation of c-Fos and microglial activation after IAMNT. When the temporal changes in activation patterns of astrocyte were compared with those of microglia, the activation of astrocytes appeared to be delayed compared to microglia (Figs. 4 and 5, Table 1).

3.5. Changes in the number of TG neurons following IAMNT

It is possible that c-Fos upregulation and the activation of glial cells in MDH can result from degenerative changes in central terminals caused by trigeminal ganglion (TG) neuronal death in response to IAMNT. Therefore, we tested whether IAMNT would result in the loss of TG neurons. When the number of Dil-labeled TG neurons whose proximal primary afferents originate from IAN and MN was monitored using retrograde labeling technique, there were no significant changes in the number of neurons by 28 days after IAMNT

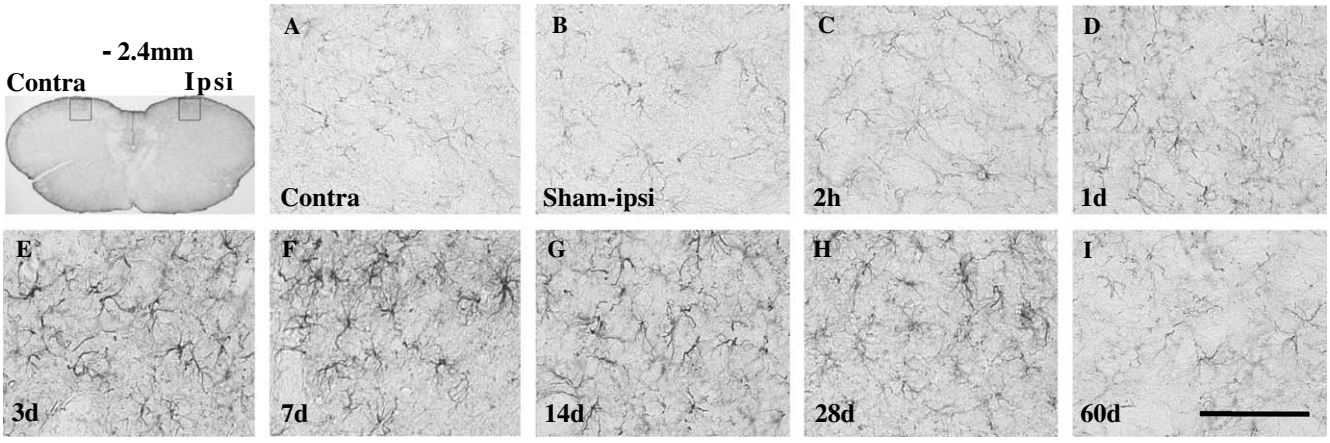

Fig. 5. GFAP-IR in the superficial laminae of the medullary dorsal horn following IAMNT at the level of 2.4 mm caudal to obex. (A–I) The magnified image of the inset indicated in left top panel. (A) Contralateral side at 7 days after IAMNT. (B) Ipsilateral side at 7 days after sham operation. (C–I) Ipsilateral side at 2 h, 1 day, 3 days, 7 days, 14 days, 28 days, and 60 days after IAMNT, respectively. GFAP-IR was very mild in the contralateral side, sham-ipsilateral side, and ipsilateral side at 2 h and 60 days after IAMNT (A–C, I), and modestly mild at 1 day after IAMNT (D). However, GFAP-IR was intense at 3, 7, and 14 days with many hypertrophic astrocytes (E–G) and moderate at 28 days after IAMNT (H). Scale bar = 100 μm.

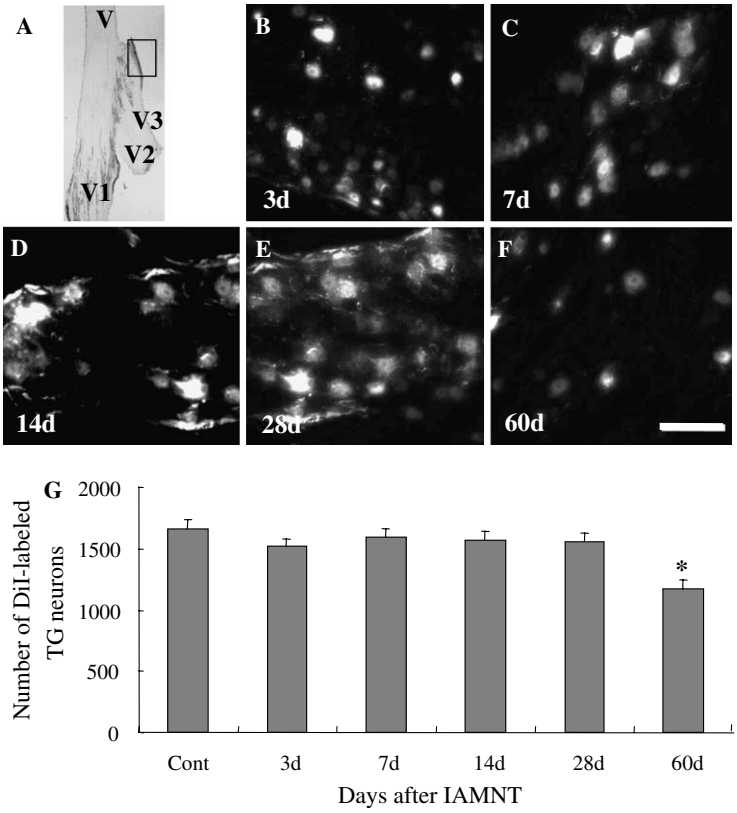

Fig. 6. Changes in the number of trigeminal ganglion (TG) neurons following IAMNT. (A) The photograph of trigeminal ganglion stained with cresyl violet. V, trigeminal nerve. VI, ophthalmic nerve. V2, maxillary nerve. V3, mandibular nerve. Rectangle indicates the areas containing DiI-labeled TG neurons which originate from IAN and MN. (B–F) Images obtained from an area inside the rectangle in A under fluorescent microscope after DiI application onto the proximal terminals to IAN and MN at 2 days before the post-surgery time points indicated in each panel. (G) Summary of the number of DiI-labeled TG neurons after IAMNT. The number of TG neurons did not change by 28 days after IAMNT (Student's *t*-test, $^{*}p < 0.05$; vs. control rats).

(Fig. 6). The number of TG neurons was decreased only at 60 days after IAMNT. This result strongly suggests that the activation of glial cells following IAMNT is not due to the degenerative changes in central terminals of primary afferents caused by TG neuronal death.

3.6. Effect of the minocycline on IAMNT-induced pain response

We confirmed in our orofacial pain model that glial activation by IAMNT correlated with the development and maintenance of pain hypersensitivity (Figs. 1, 4, and 5). We therefore investigated whether IAMNT-induced neuropathic pain could be decreased by the inhibition of microglial activation in MDH. We used minocycline as an inhibitor of microglial activation. The dosage of minocycline (15 or 30 mg/kg) was determined based on the previous reports which demonstrated therapeutic effects of minocycline (Yrjanheikki et al., 1998; Wu et al., 2002; Zhu et al., 2002; Raghavendra et al., 2003; Zhang et al., 2003.) As shown in Fig. 7, minocycline treatment significantly decreased the pain hypersensitivity following IAMNT in a dose-dependent manner. At 1 day after IAMNT, the relative escape thresholds in the ipsilateral side of minocycline (30 mg/kg)-treated rats increased to 76% of pre-operative level, compared to those (39% of pre-operative level) of saline-treated rats. The enhancement of escape thresholds in minocycline-treated rats was still significant by 28 days following IAMNT, but the threshold returned to the pre-operative level at 60 days after IAMNT. 15 mg/kg of minocycline showed a similar time course of escape thresholds, but with lesser effect than 30 mg/kg minocycline. When we tested the relative escape thresholds in the contralateral side of minocycline-treated rats, the escape thresholds to mechanical stimulation were approximately similar to those of saline-treated rats.

3.7. Attenuation of IAMNT-induced pain hypersensitivity by minocycline correlates with inhibition of MDH glial p38 MAPK

Minocycline, an inhibitor of microglial activation, produced its neuroprotective effects by inhibiting microglial p38 mitogen-activated protein kinase (MAPK)

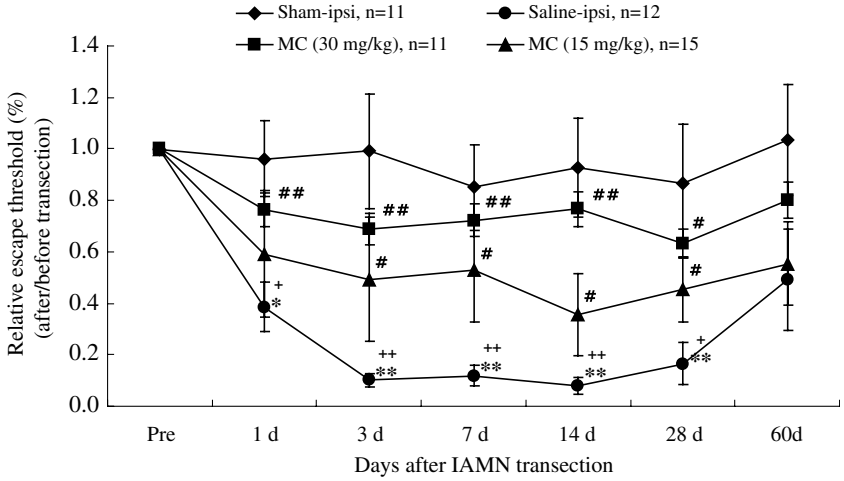

Fig. 7. Effects of minocycline (15 or 30 mg/kg) on pain hypersensitivity in response to the mechanical stimulation in the whisker pad area after IAMNT. Sham-ipsi, ipsilateral side to sham-operated rats; IAMNT-ipsi, ipsilateral side to saline-treated rats; MC-ipsi, ipsilateral side to minocycline-treated rats. The decrease of escape threshold to the application of von Frey filament by IAMNT was significantly prevented in the minocycline-treated rats at post- 1–28 days after IAMNT (Newman–Keuls test; $^{*,\#,+}p < 0.05$; $^{**,\#\#,++}p < 0.01$; *, saline-ipsi vs. pre-operative (Pre); #, MC-ipsi vs. saline-ipsi; +, saline-ipsi vs. sham-ipsi).

phosphorylation in a model of Parkinson's disease (Du et al., 2001) and in neurons exposed to glutamate or NMDA (Tikka and Koistinaho, 2001; Tikka et al., 2001). We examined whether p38 MAPK pathways would mediate the inhibitory effect of minocycline on pain hypersensitivity in IAMNT rats using immunofluorescence analysis (Fig. 8). We found that a phosphorylated form of p38 MAPK (p-p38 MAPK) was increased in the MDH ipsilateral to nerve injury (Fig. 8D). Interestingly, the p-p38 MAPK immunofluorescence in the dorsal horn was found exclusively in activated microglia (Figs. 8D–F), but not in neurons (Figs. 8J–L) or astrocytes (Figs. 8M–O). The level of p-p38 MAPK immunofluorescence in individual microglial cells was much higher in the ipsilateral dorsal horn compared to the contralateral side (Figs. 8A–F). No immunoreactivity was detected when the primary antibody was omitted. When examined at 3 days, the time point where microglia were maximally activated by IAMNT (Fig. 4) and minocycline produced the maximal inhibitory effects on pain hypersensitivity (Fig. 7), phosphorylation of p38 MAPK and microglial activation were decreased by minocycline (30 mg/kg, i.p.) (Figs. 8G–I).

4. Discussion

The aim of this study was to investigate whether glial cell activation in MDH would contribute to trigeminal neuropathic pain. Following transection of the inferior alveolar nerve and the mental nerve, rats showed tactile hypersensitivity on the whisker pad area, as manifested by the decrease of tactile threshold in response to the application of von Frey filaments. In these IAMNT rats, we found early enhancement of c-Fos immunoreactivity, followed by microglial and astrocytic activation in MDH. The glial activation was correlated with the development and maintenance of tactile hypersensitivity following IAMNT. Minocycline reduced microglial activation, inhibited p38 MAPK activation in microglia, and significantly attenuated the development of pain hypersensitivity in our trigeminal neuropathic pain model.

4.1. Effect of IAMNT on c-Fos protein expression

The expression of Fos protein has been widely used as a marker for neuronal activation in CNS including somatosensory system (Curran and Morgan, 1995). Indeed, it has been demonstrated that c-Fos-IR is enhanced in MDH neurons, in response to peripheral insults such as injury to trigeminal nerve (Terayama et al., 1997; Nomura et al., 2002), noxious stimulation (Strassman et al., 1993) or orofacial inflammation (Gojyo et al., 2002). In agreement with a previous report (Nomura et al., 2002), the increase in IAMNT-induced c-Fos-IR was mainly observed in the superficial laminae (I–II) of MDH where the primary nociceptive afferents from mandibular nerve terminate. However, unlike the report by Nomura et al. (2002), in which only inferior alveolar nerve was transected, the enhancement of c-Fos expression following IAMNT was clearly observed even without mechanical stimulation. This might be due to the difference in the severity of peripheral injury employed in our study. IAMNT might result in excessive release of neurotransmitters from primary afferents (Watkins and Maier, 2003) and degenerative or regenerative changes in the central terminals of inferior alveolar nerve and mental nerve (Cameron et al., 1997). As expected, the c-Fos expression in MDH neurons was an immediate early response, peaking at 2 h and 1 day after IAMNT, although the enhancement of c-Fos expression lasted until 14 days after IAMNT

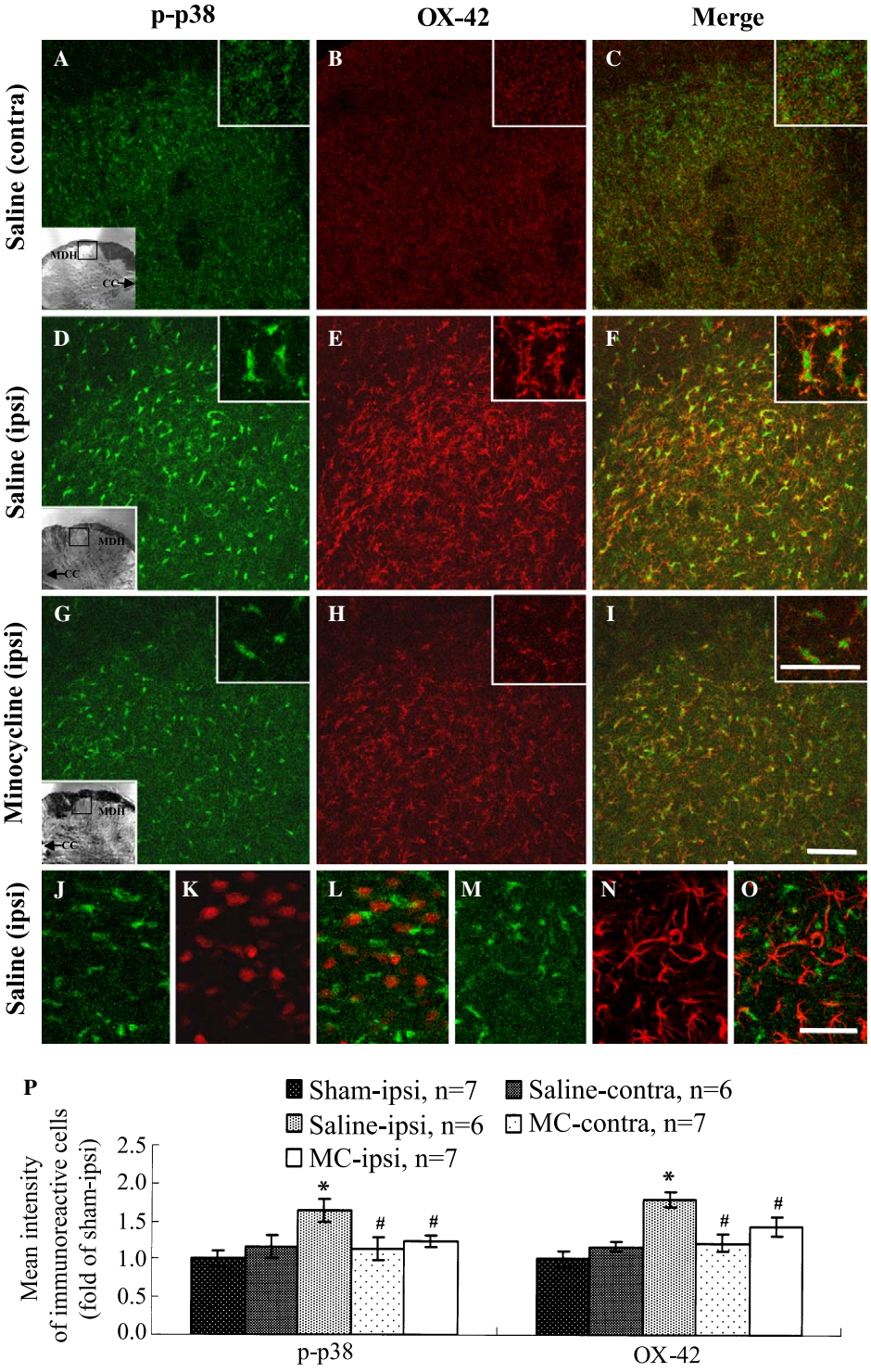

Fig. 8. Phospho-p38 (p-p38) MAPK and OX-42 IR in the medial portion of the superficial laminae of the MDH at 3 days after IAMNT at the level of 2.4 mm caudal to obex. While p-p38 MAPK-IR and OX-42 IR were increased in the MDH following nerve injury, the immunointensities of p-p38 MAPK and OX-42 were reduced by minocycline treatment (30 mg/kg, i.p.). (A, D, and G, p-p38 MAPK, green color; B, E, H, OX-42, red color). The p-p38 MAPK immunofluorescence was found exclusively in activated microglia (C, F, I; merged image), but not in neurons (J, p-p38 MAPK; K, NeuN; L, merged image) or astrocytes (M, p-p38 MAPK; N, GFAP; O, merged image). (A–C) Contralateral side to saline-treated rats, (D–F) ipsilateral side to saline-treated rats, and (G–I) ipsilateral side to minocycline-treated rats. MDH, medullary dorsal horn; CC, central canal. Insets of right upper corner are high magnification images. Bar = 50 μm. (P) The p-p38 and OX-42 IR intensity was measured as the average pixel intensity per 0.5 mm^2 area within medial portion of the MDH at the level of 2.4 mm caudal to obex at 3 days after IAMNT. The p-p38 and OX-42 IR intensity was significantly decreased by minocycline (Newman–Keuls test; $^{*}p < 0.01$; vs. ipsilateral of sham-treated rats/contralateral of saline-treated rats; $^{\#}P < 0.01$; vs. ipsilateral of saline-treated rats).

(Fig. 3). Because c-Fos plays a key role in regulation of transcription of several genes including tumor necrosis factor (TNF)-α which is believed to activate glial cells (Schafers et al., 2003a,b; Ohtori et al., 2004), the consequence of c-Fos induction in MDH neurons might be important for the sequential activation of glial cells. In line with this possibility, a recent report demonstrated that sequential activation of microglia and astrocytes follows early transient activation of neurons in spinal nerve ligation model (Zhuang et al., 2005). The degenerative changes in the central terminals of primary afferents caused by neuronal death from IAMNT seem not to contribute to changes in c-Fos expression, as we found that the number of TG neurons did not change after IAMNT by 28 days (Fig. 6).

4.2. Effect of IAMNT on glial activation in MDH

Previous studies reported that microglia and astrocytes are activated by peripheral insults such as peripheral nerve injury (Garrison et al., 1991; Kalla et al., 2001) and peripheral inflammation (Fu et al., 1999), and the spinal glial activation might be a causal factor in the pain hypersensitivity at the spinal level (Watkins et al., 2001). Consistent with these studies, glial activation was also induced in our orofacial neuropathic pain model. The locations showing the greatest number of activated glia corresponded approximately to the area of MDH where we observed c-Fos upregulation. Therefore, it seems reasonable to speculate that substances released from nociceptive afferents and/or MDH neurons, or inflammatory response due to the degenerative changes of central terminals, in response to the IAMNT, might play important roles in the activation of glial cells. However, little was known yet as to which is the major factor for glial activation and what substances activate glial cells. However, since we found that the loss of TG neurons was not significant by 28 day following IAMNT (Fig. 6), it is likely that the glial activation is due to the substances released from primary afferents and/or MDH neurons rather than the degenerative changes of central terminals.

Recently, ATP and fractalkine were suggested as plausible candidates which activate glial cells (Tsuda et al., 2003; Wieseler-Frank et al., 2004). Tsuda et al. (2003) have demonstrated P2X4 upregulation by the activated microglia following spinal nerve injury and the inhibition of neuropathic pain by P2X antagonist, suggesting that extracellular ATP might be one of the critical mediators for the development of neuropathic pain. We also found significant increase in the production of proinflammatory cytokines by ATP in in vitro study using spinal glial cultures (unpublished observation). Fractalkine from primary afferents is another candidate molecule (Wieseler-Frank et al., 2004). Fractalkine, which is known to mediate neuron-to-glia interaction in the CNS, has been reported to induce allodynia and hyperalgesia through CX3CR1, the only known fractalkine receptor. Endogenous toll-like receptor ligands such as heat-shock proteins also may contribute to glial activation (Tanga et al., 2005).

It was interesting to note that temporal changes in the activation of microglia are different from those of astrocytes. As indicated in Table 1, microglia was likely to be activated and return to the basal level earlier than astrocytes. In the CNS, microglia are the initial responders to insults such as trauma, ischemia, tumors, and inflammation (Kreutzberg, 1996). Furthermore, as a consequence of peripheral insults such as facial nerve injury, sciatic nerve injury, and inflammation, and microglia were reported to become rapidly activated, which is followed by delayed astrocytic activation (Sweitzer et al., 1999). Therefore, it is likely that microglia initially activated by IAMNT also lead to the activation of astrocytes and they then communicate with each other to activate back and forth via autocrine or paracrine actions. Consistent with this is our finding that the development of neuropathic pain was attenuated by minocycline, an inhibitor of microglia (Fig. 7). However, it is possible that upon excessive neuronal stimulation astrocytes release a microglial activating factor (e.g., ATP) which initiates the paracrine cascade of mutual activation (Bianco et al., 2005).

4.3. Physiological implication

It is becoming clear that glial activation following sensory nerve injury is a critical factor for the exaggerated pain response (Watkins and Maier, 2002, 2003; Zhuang et al., 2005). Recent studies provide significant evidence that activated spinal glia release mediators that act on other glia and neurons, thereby either enhancing neurotransmitter release from primary afferents or causing hyperexcitability of pain transmitting neurons (Watkins and Maier, 2002, 2003). All these results support the notion that spinal glial cell activation is not just the passive response from peripheral insults to the spinal sensory nerve. We propose that this is similar in the trigeminal system. Tactile hypersensitivity in response to the IAMNT has been found to clearly correlate with the temporal changes in the activation of microglia and astrocytes (Figs. 1, 4, and 5, Table 1). Our behavioral data strongly suggest that MDH glial activation might regulate pain hypersensitivity following peripheral nerve injury in the trigeminal system as spinal glial cells do at the spinal level.

The precise signaling pathways within activated glia following peripheral nerve injury are poorly understood yet. Since minocycline inhibited tactile hypersensitivity (Fig. 7) and p38 MAPK activation in MDH hyperactive microglia (Fig. 8), p38 activation seems to contribute to the development of neuropathic pain, as at spinal level (Tsuda et al., 2004). p38 activation regulates the expression of cytokines, cyclooxygenase (COX)-2, and

inducible nitric oxide synthase (iNOS), thereby leading to the synthesis of prostaglandin and nitric oxide, which can also enhance pain sensitivity (Jin et al., 2003). Activated microglia are also known to release substances such as pro-inflammatory cytokines (including interleukin-1β (IL-1β), IL-6, and TNF-α) (Hanisch, 2002), excitatory amino acids (EAAs), and reactive oxygen species (ROS), that can contribute to different features of pathological pain (Watkins and Maier, 2002; Ledeboer et al., 2005). Minocycline has been shown to reduce microglia activation and levels of IL-1β, NO, and prostaglandin release likely through inhibition of p38 MAPK activation (Stirling et al., 2005). However, although minocycline greatly reduced p38 MAPK mRNA level, and MAPKK3 and MAPKK6 have been suggested as targets of minocycline, the exact upstream targets are still unknown (Stirling et al., 2005). In addition, minocycline inhibits nuclear factor (NF)-κB activation in microglia (Si et al., 2004) and phospholipase A2 activity in vitro (Pruzanski et al., 1992). Minocycline also reduces migration of immune cells through inhibition of matrix metalloproteinases (Brundula et al., 2002) and by altering levels of chemokines and/or chemokine receptor expression (Kremlev et al., 2004). These mechanisms may underlie the inhibition of pain hypersensitivity by minocycline in our study.

In summary, IAMNT rat generated in this study provides a valid model for trigeminal neuropathic pain with tactile hypersensitivity. Glial activation has a substantial role in pain hypersensitivity following peripheral nerve injury in the trigeminal system. Glial activation might not result from degenerative changes in central terminals of primary afferents caused by the neuronal death. Activation of p38 MAPK in MDH hyperactive microglia is likely to contribute to pain hypersensitivity following peripheral nerve injury.

Acknowledgments

I thank Dr. RA North in University of Manchester, UK, for his valuable comments and English corrections of the manuscript. This research was supported by grant (M103KV010009-04K2201-00930) from Brain Research Center of the 21st Century Frontier Research Program funded by the Ministry of Science and Technology and grant (RO1-2004-000-103 84-0) from the Basic Research Program of the Korea Science & Engineering Foundation, Republic of Korea.

Appendix A. Supplementary data

Supplementary data associated with this article can be found, in the online version, at doi:10.1016/j.pain.2005.12.023.

References

Aschner M. Astrocytes as mediators of immune and inflammatory responses in the CNS. Neurotoxicology 1998;19(2):269–81.

Bianco F, Pravettoni E, Colombo A, Schenk U, Moller T, Matteoli M, et al. Astrocyte-derived ATP induces vesicle shedding and IL-1 beta release from microglia. J Immunol 2005;174(11):7268–77.

Brundula V, Rewcastle NB, Metz LM, Bernard CC, Yong VW. Targeting leukocyte MMPs and transmigration: minocycline as a potential therapy for multiple sclerosis. Brain 2002;125(Pt 6):1297–308.

Bursztajn S, Rutkowski MD, Deleo JA. The role of the *N*-methyl-D-aspartate receptor NR1 subunit in peripheral nerve injury-induced mechanical allodynia, glial activation and chemokine expression in the mouse. Neuroscience 2004;125(1):269–75.

Cameron AA, Cliffer KD, Dougherty PM, Garrison CJ, Willis WD, Carlton SM. Time course of degenerative and regenerative changes in the dorsal horn in a rat model of peripheral neuropathy. J Comp Neurol 1997;379(3):428–42.

Colburn RW, DeLeo JA, Rickman AJ, Yeager MP, Kwon P, Hickey WF. Dissociation of microglial activation and neuropathic pain behaviors following peripheral nerve injury in the rat. J Neuroimmunol 1997;79(2):163–75.

Curran T, Morgan JI. Fos: an immediate-early transcription factor in neurons. J Neurobiol 1995;26(3):403–12.

DeLeo JA, Winkelstein BA. Physiology of chronic spinal pain syndromes: from animal models to biomechanics. Spine 2002;27(22):2526–37.

Du Y, Ma Z, Lin S, Dodel RC, Gao F, Bales KR, et al. Minocycline prevents nigrostriatal dopaminergic neurodegeneration in the MPTP model of Parkinson's disease. Proc Natl Acad Sci USA 2001;98(25):14669–74.

Fu KY, Light AR, Matsushima GK, Maixner W. Microglial reactions after subcutaneous formalin injection into the rat hind paw. Brain Res 1999;825(1–2):59–67.

Garrison CJ, Dougherty PM, Kajander KC, Carlton SM. Staining of glial fibrillary acidic protein (GFAP) in lumbar spinal cord increases following a sciatic nerve constriction injury. Brain Res 1991;565(1):1–7.

Gojyo F, Sugiyo S, Kuroda R, Kawabata A, Varathan V, Shigenaga Y, et al. Effects of somatosensory cortical stimulation on expression of c-Fos in rat medullary dorsal horn in response to formalin-induced noxious stimulation. J Neurosci Res 2002;68(4):479–88.

Hanisch UK. Microglia as a source and target of cytokines. Glia 2002;40(2):140–55.

Inoue K, Koizumi S, Tsuda M, Shigemoto-Mogami Y. Signaling of ATP receptors in glia-neuron interaction and pain. Life Sci 2003;74(2–3):189–97.

Jin SX, Zhuang ZY, Woolf CJ, Ji RR. p38 mitogen-activated protein kinase is activated after a spinal nerve ligation in spinal cord microglia and dorsal root ganglion neurons and contributes to the generation of neuropathic pain. J Neurosci 2003;23(10):4017–22.

Kalla R, Liu Z, Xu S, Koppius A, Imai Y, Kloss CU, Kohsaka S, Gschwendtner A, Moller JC, Werner A, Raivich G. Microglia and the early phase of immune surveillance in the axotomized facial motor nucleus: impaired microglial activation and lymphocyte recruitment but no effect on neuronal survival or axonal regeneration in macrophage-colony stimulating factor-deficient mice. J Comp Neurol 2001;436(2):182–201.

Kremlev SG, Roberts RL, Palmer C. Differential expression of chemokines and chemokine receptors during microglial activation and inhibition. J Neuroimmunol 2004;149(1–2):1–9.

Kreutzberg GW. Microglia: a sensor for pathological events in the CNS. Trends Neurosci 1996;19(8):312–8.

Ledeboer A, Sloane EM, Milligan ED, Frank MG, Mahony JH, Maier SF, Watkins LR. Minocycline attenuates mechanical allodynia and proinflammatory cytokine expression in rat models of pain facilitation. Pain 2005;115(1–2):71–83.

Nomura H, Ogawa A, Tashiro A, Morimoto T, Hu JW, Iwata K. Induction of Fos protein-like immunoreactivity in the trigeminal spinal nucleus caudalis and upper cervical cord following noxious and non-noxious mechanical stimulation of the whisker pad of the rat with an inferior alveolar nerve transection. Pain 2002;95(3):225–38.

Ohtori S, Takahashi K, Moriya H, Myers RR. TNF-alpha and TNF-alpha receptor type 1 upregulation in glia and neurons after peripheral nerve injury: studies in murine DRG and spinal cord. Spine 2004;29(10):1082–8.

Pruzanski W, Greenwald RA, Street IP, Laliberte F, Stefanski E, Vadas P. Inhibition of enzymatic activity of phospholipases A2 by minocycline and doxycycline. Biochem Pharmacol 1992;44(6):1165–70.

Raghavendra V, Tanga F, DeLeo JA. Inhibition of microglial activation attenuates the development but not existing hypersensitivity in a rat model of neuropathy. J Pharmacol Exp Ther 2003;306(2):624–30.

Schafers M, Lee DH, Brors D, Yaksh TL, Sorkin LS. Increased sensitivity of injured and adjacent uninjured rat primary sensory neurons to exogenous tumor necrosis factor-alpha after spinal nerve ligation. J Neurosci 2003a;23(7):3028–38.

Schafers M, Svensson CI, Sommer C, Sorkin LS. Tumor necrosis factor-alpha induces mechanical allodynia after spinal nerve ligation by activation of p38 MAPK in primary sensory neurons. J Neurosci 2003b;23(7):2517–21.

Si Q, Cosenza M, Kim MO, Zhao ML, Brownlee M, Goldstein H, et al. A novel action of minocycline: inhibition of human immunodeficiency virus type 1 infection in microglia. J Neurovirol 2004;10(5):284–92.

Stirling DP, Koochesfahani KM, Steeves JD, Tetzlaff W. Minocycline as a neuroprotective agent. Neuroscientist 2005;11(4):308–22.

Strassman AM, Vos BP. Somatotopic and laminar organization of fos-like immunoreactivity in the medullary and upper cervical dorsal horn induced by noxious facial stimulation in the rat. J Comp Neurol 1993;331(4):495–516.

Strassman AM, Vos BP, Mineta Y, Naderi S, Borsook D, Burstein R. Fos-like immunoreactivity in the superficial medullary dorsal horn induced by noxious and innocuous thermal stimulation of facial skin in the rat. J Neurophysiol 1993;70(5):1811–21.

Sweet WH. Deafferentation pain after posterior rhizotomy, trauma to a limb, and herpes zoster. Neurosurgery 1984;15(6):928–32.

Sweitzer SM, Colburn RW, Rutkowski M, DeLeo JA. Acute peripheral inflammation induces moderate glial activation and spinal IL-lbeta expression that correlates with pain behavior in the rat. Brain Res 1999;829(1–2):209–21.

Tanga FY, Nutile-McMenemy N, DeLeo JA. The CNS role of Toll-like receptor 4 in innate neuroimmunity and painful neuropathy. Proc Natl Acad Sci USA 2005;102(16):5856–61.

Terayama R, Nagamatsu N, Ikeda T, Nakamura T, Rahman OI, Sakoda S, Shiba R, Nishimori T. Differential expression of Fos protein after transection of the rat infraorbital nerve in the trigeminal nucleus caudalis. Brain Res 1997;768(1–2):135–46.

Tikka T, Fiebich BL, Goldsteins G, Keinanen R, Koistinaho J. Minocycline, a tetracycline derivative, is neuroprotective against excitotoxicity by inhibiting activation and proliferation of microglia. J Neurosci 2001;21(8):2580–8.

Tikka TM, Koistinaho JE. Minocycline provides neuroprotection against *N*-methyl-D-aspartate neurotoxicity by inhibiting microglia. J Immunol 2001;166(12):7527–33.

Tsuda M, Inoue K, Salter MW. Neuropathic pain and spinal microglia: a big problem from molecules in "small" glia. Trends Neurosci 2005;28(2):101–7.

Tsuda M, Mizokoshi A, Shigemoto-Mogami Y, Koizumi S, Inoue K. Activation of p38 mitogen-activated protein kinase in spinal hyperactive microglia contributes to pain hypersensitivity following peripheral nerve injury. Glia 2004;45(1):89–95.

Tsuda M, Shigemoto-Mogami Y, Koizumi S, Mizokoshi A, Kohsaka S, Salter MW, Inoue K. P2X4 receptors induced in spinal microglia gate tactile allodynia after nerve injury. Nature 2003;424(6950):778–83.

Vos BP, Strassman AM, Maciewicz RJ. Behavioral evidence of trigeminal neuropathic pain following chronic constriction injury to the rat's infraorbital nerve. J Neurosci 1994;14(5 Pt 1):2708–23.

Watkins LR, Maier SF. Beyond neurons: evidence that immune and glial cells contribute to pathological pain states. Physiol Rev 2002;82(4):981–1011.

Watkins LR, Maier SF. Glia: a novel drug discovery target for clinical pain. Nat Rev Drug Discov 2003;2(12):973–85.

Watkins LR, Milligan ED, Maier SF. Glial activation: a driving force for pathological pain. Trends Neurosci 2001;24(8):450–5.

Wieseler-Frank J, Maier SF, Watkins LR. Glial activation and pathological pain. Neurochem Int 2004;45(2–3):389–95.

Winkelstein BA, DeLeo JA. Nerve root injury severity differentially modulates spinal glial activation in a rat lumbar radiculopathy model: considerations for persistent pain. Brain Res 2002;956(2):294–301.

Wu DC, Jackson-Lewis V, Vila M, Tieu K, Teismann P, Vadseth C, et al. Blockade of microglial activation is neuroprotective in the 1-methyl-4-phenyl-1,2,3,6-tetrahydropyridine mouse model of Parkinson disease. J Neurosci 2002;22(5):1763–71.

Yonehara N, Kudo C, Kamisaki Y. Involvement of NMDA-nitric oxide pathways in the development of tactile hypersensitivity evoked by the loose-ligation of inferior alveolar nerves in rats. Brain Res 2003;963(1–2):232–43.

Yrjanheikki J, Keinanen R, Pellikka M, Hokfelt T, Koistinaho J. Tetracyclines inhibit microglial activation and are neuro protective in global brain ischemia. Proc Natl Acad Sci USA 1998;95(26):15769–74.

Zhang SC, Goetz BD, Duncan ID. Suppression of activated microglia promotes survival and function of transplanted oligodendroglial progenitors. Glia 2003;41(2):191–8.

Zhu S, Stavrovskaya IG, Drozda M, Kim BY, Ona V, Li M, et al. Minocycline inhibits cytochrome c release and delays progression of amyotrophic lateral sclerosis in mice. Nature 2002;417(6884):74–8.

Zhuang ZY, Gerner P, Woolf CJ, Ji RR. ERK is sequentially activated in neurons, microglia, and astrocytes by spinal nerve ligation and contributes to mechanical allodynia in this neuropathic pain model. Pain 2005;114(1–2):149–59.

Zimmermann M. Ethical guidelines for investigations of experimental pain in conscious animals. Pain 1983;16(2):109–10.

Zimmermann M. Pathobiology of neuropathic pain. Eur J Pharmacol 2001;429(1–3):23–37.